Journal of Colloid and Interface Science 428 (2014) 8–15

Contents lists available at ScienceDirect

Journal of Colloid and Interface Science

www.elsevier.com/locate/jcis

Effect of annealing on the structural, morphological and photoluminescence properties of ZnO thin films prepared by spin coating

Vinod Kumar [a], Vijay Kumar [a], S. Som [a], A. Yousif [a], Neetu Singh [b,c], O.M. Ntwaeaborwa [a], Avinashi Kapoor [b], H.C. Swart [a,*]

[a] Department of Physics, University of the Free State, Bloemfontein, ZA 9300, South Africa
[b] Department of Electronic Science, University of Delhi South Campus, New Delhi 110 021, India
[c] Department of Electronics, Keshav Mahavidyalaya, University of Delhi, Delhi 110 034, India

ARTICLE INFO

Article history:
Received 25 February 2014
Accepted 14 April 2014
Available online 24 April 2014

Keywords:
Annealing time
ZnO thin films
Spin coating
Sol–gel
Auger electron spectroscopy

ABSTRACT

Zinc oxide (ZnO) thin films were deposited on silicon substrates by a sol–gel method using the spin coating technique. The ZnO films were annealed at 700 °C in an oxygen environment using different annealing times ranging from 1 to 4 h. It was observed that all the annealed films exhibited a hexagonal wurtzite structure. The particle size increased from 65 to 160 nm with the increase in annealing time, while the roughness of the films increased from 2.3 to 10.6 nm with the increase in the annealing time. Si diffusion from the substrate into the ZnO layer occurred during the annealing process. It is likely that the Si and O_2 influenced the emission of the ZnO by reducing the amount of Zn defects and the creation of new oxygen related defects during annealing in the O_2 atmosphere. The emission intensity was found to be dependent on the reflectance of the thin films.

1. Introduction

Zinc oxide (ZnO) thin films have attracted much attention from the research community due to its fascinating optical and electrical properties. ZnO is a groups II–VI semiconductor compound which has many attractive potential applications in the field of optoelectronics such as light emitting diodes (LEDs) [1], electroluminescence devices [2] and solar cells [3,4] and bio-medical applications [5]. Furthermore, ZnO is inexpensive, chemically stable, easy to prepare and etch, and nontoxic, which also make the fabrication of ZnO-based optical devices an attractive prospect. However, contradicted statements are found. Some found ZnO an attractive prospect while Pearton and Ren [6] concluded that the future for commercial ZnO light emitters looks quite bleak, given the lack of real progress in the past 5 years. They proposed that at this stage, the best approach may be a continued effort on the growth process of these materials, leading to a better understanding of dopant incorporation and defect control. The understanding of native defects in ZnO is still far from complete and has been largely driven by first principal calculations using different approaches. Most of the previous studies on p-type ZnO have focused on addressing the low solubility and the high ionization energy of the acceptors. Recently, the fabrication of p-type ZnO has made great progress by mono-doping group V elements (N, P, As, and Sb) and co-doping III–V elements with various technologies, such as ion implantation, pulsed laser deposition (PLD), and molecular beam epitaxy (MBE) [7,8]. Various authors reported optically pumped UV lasing of ZnO films grown by molecular beam epitaxy (MBE) and pulsed laser deposition (PLD) [9–11]. This makes ZnO a potential competitor of Gallium nitrate (GaN). ZnO has not only the same crystal structure as GaN, but also a larger exciton binding energy of 60 meV, which is 2.4 times that of GaN. Furthermore, Yu et al. have reported that textured ZnO films might have higher quantum efficiency than GaN [12]. This indicates that ZnO is the material with the most potential to be realized as the next generation of UV semiconductor laser. Silicon (Si) is not only of interest for the integration of opto-electronic devices but is also cheaper and easier to cleave in comparison with sapphire, which is widely used as substrate in the deposition of ZnO films [13,14]. Several reports have addressed the difficulties in the fabrication of ZnO thin films based on the opto-electronic devices as a result of factors such as surface morphology, hydroxide formation, carbon contamination, and subsurface defects and impurities [15,16]. The large lattice mismatch and a

* Corresponding author. Fax: +27 514013507.
E-mail addresses: vinod.phy@gmail.com (V. Kumar), swarthc@ufs.ac.za (H.C. Swart).

http://dx.doi.org/10.1016/j.jcis.2014.04.035
0021-9797/

large difference in the thermal expansion coefficients between ZnO films and Si substrates cause built-in residual stress in the deposited ZnO films [17,18]. The mismatch between ZnO and Si can be reduced by thermal annealing, thereby improving the degree of crystallinity as well. The effect of annealing temperature on the properties of ZnO thin films has been reported by several research groups [19–23], while very few researchers have reported the role of annealing time [24,25].

In order to reduce the mismatch between ZnO and Si and to dope the ZnO with Si the effect of annealing times on the structure, morphology and luminescence properties of ZnO films grown on Si substrates were investigated and is presented. A grain growth mechanism relating to longer annealing times and the possible influence of Si diffusion on the luminescence are discussed.

2. Experimental details

Thin films of ZnO synthesized via the sol–gel method were spin-coated on Si (100) substrate. For the synthesis of ZnO, zinc acetate dihydrate (Alfa Aesar) was used as the zinc source. Methanol (AR, Merck) and monoethanolamine (MEA, Merck) were used as solvent and stabilizer, respectively. The zinc precursor solution of concentration 0.2 mol/l was prepared by dissolving zinc acetate dihydrate in methanol. MEA was then added into the solution. The molar ratio of the MEA/Zinc solution was fixed at 1. The above solution was stirred using a magnetic stirrer at 50 °C for 30 min. The optimization and other synthesis details have been reported elsewhere [4]. The Si substrates were first cleaned in a boiling mixture of NH_4OH:H_2O_2:H_2O in the ratio of 1:1:6 for approximately 10 min. The substrates were then rinsed in deionized water for 10 min and were later treated with 2% HF solution to remove the native oxide. They were further washed with deionized water for 20 min and were dried in nitrogen atmosphere. The solution was then spin coated onto the Si substrates, which were rotated at 2500 r/min for 30 s. The films were dried in air at 230 °C for 10 min on a hot plate. The procedure from coating to drying was repeated 8 times. The ZnO/Si films were kept in a microprocessor controlled furnace and annealed in an oxygen flowing atmosphere at an annealing temperature of 700 °C for different annealing times ranging from 1 to 4 h. The structure of the films was analyzed with an Advanced D8 Bruker powder diffractometer with a Cu anode X-ray tube (with a K_α radiation wavelength of 1.54 Å). The surface morphology and roughness were examined from images captured in the contact mode using a Shimadzu SPM-9600 atomic force microscope (AFM). The root mean square (RMS) roughnesses were estimated by analyzing the topography scans of the films surfaces using commercially available software. A PHI 700 nanoprobe was used to make depth profiles of the thin films. A 25 keV, 10 nA electron beam was used. The Auger peak to peak heights (APPH's) were monitored while sputtering with 2 keV, 2 mA Ar^+ ions using a raster that scanned the Ar^+ ion beam over a 2×2 mm^2 area and the sputtering rate was 8.5 nm per minute. Photoluminescence (PL) data were recorded using a He–Cd laser with a 325 nm excitation wavelength. All measurements were taken at room temperature.

3. Results and discussion

3.1. Structural analysis

Fig. 1(a) shows the XRD patterns of the as-prepared ZnO film as well as the films after annealed for different annealing times. The XRD pattern of the as-prepared thin film shows that the film has an amorphous nature, while the annealed films have a hexagonal wurtzite structure and most of the crystallites were having a strong *c*-axis orientation along the (002) plane. Besides this there

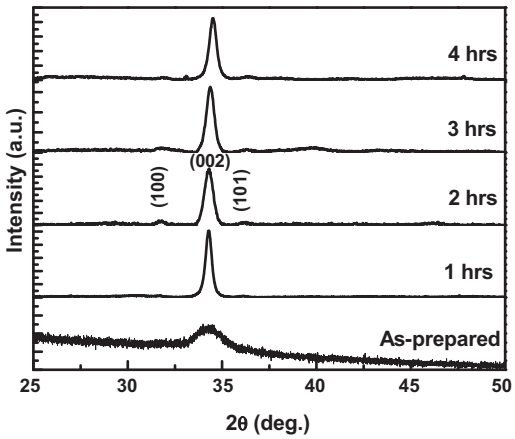

Fig. 1. XRD patterns of ZnO film as-prepared and different annealing times.

are other very small diffraction peaks also corresponding to the (100) and (101) of ZnO. The increase in annealing time improved the stoichiometry of the films and the crystal quality [19].

The crystallite sizes of the ZnO were calculated using the full width at half maxima (FWHM) of the (002) peak using Scherer's formula given below [26]

$$D = \frac{K\lambda}{\beta \cos\theta} \tag{1}$$

where D is the size of the crystallites, λ is the wavelength of Cu kα radiation (0.1514 Å), k is correlation factor (0.94), β is FWHM of (002) peak and θ is Bragg's diffraction angle. The crystallite sizes varied from 18 to 25 nm with increasing annealing time, while it was 6 nm for the as-prepared thin film. The numerical values of the lattice spacing for the ZnO films were also calculated, Table 1, from the XRD data according to the following equations [27]

$$2d_{hkl} \sin\theta = n\lambda \tag{2}$$

where d_{hkl} is lattice spacing of (hkl) and θ is the Bragg angle (half of the peak position angle). For the wurtzite structure the interplanar distance of the (hkl) plane is related to the lattice parameters a and c via the Miller indices hkl.

$$\left(\frac{1}{d_{hk}}\right)^2 = \frac{4}{3}\left(\frac{h^2 + k^2 + hk}{a^2}\right) + \frac{l^2}{C^2} \tag{3}$$

where a and c are the lattice constants; h, k, l are Miller indices. With the first order approximation $n = 1$, the lattice constant a was calculated by [28]

$$a = \frac{\lambda}{\sqrt{3}\sin\theta} \tag{4}$$

For the (002) plane, the lattice constant c was calculated by

$$c = \frac{\lambda}{\sin\theta} \tag{5}$$

Table 1
Effect of annealing time on the structural parameter calculated using XRD results.

Annealing time (h)	2θ (deg.)	Stress (GPa)	Lattice constant 'c'	Lattice constant 'a'
As-prepared	34.235	−2.73	5.2368	3.2069
1	34.287	−2.05	5.2290	3.2021
2	34.296	−1.93	5.2277	3.2013
3	34.375	−0.924	5.2161	3.1941
4	34.518	0.906	5.1951	3.1813